# DETERMINATION OF INTERFACIAL FRACTURE TOUGHNESS FROM THE FRAGMENTATION TEST DATA BY VARIATIONAL MODELS

W. Wu[1], I. Verpoest[1], J. Varna[2]

[1]*Department of Metallurgy and Materials Engineering, Katholieke Universiteit Leuven De Croylaan 2, 3001 Heverlee, Belgium*
[2]*Department of Materials and Production Engineering, Lulea University of Technology, S-97187 Lulea, Sweden*

**SUMMARY:** The single fibre fragmentation test is commonly used to characterise the interfacial properties, a.o. the interfacial fracture toughness. Fibre fracture in the fragmentation test is, in many fibre-matrix systems, followed by debonding at the interface. The debonded interface is under radial compression due to residual strain and a mismatch in Poisson's ratios. The debond crack surfaces are hence in contact and the debond crack propagation is pure mode II. Two previously derived, rigorous stress-based variational models, associated with a recently derived expression for the energy release rate due to a frictional crack growth, have been applied to the fragmentation test data to calculate the values of interfacial fracture toughness for two and three phase systems. It was found that the calculated values of interfacial fracture toughness are profoundly influenced by the value of the friction coefficient at the debonded interface and the accuracy of the used model.

**KEYWORDS: variational models, interface debonding, friction work at rough crack, perturbation stresses, complementary energy, energy release rate, interfacial fracture toughness, fragmentation test data**

## INTRODUCTION

The commonly used interface failure criteria are based on a strength or fracture mechanics approach. The fracture mechanics approach appears to be more appropriate for analysing the failure with singularities and a multi-axial stress state. It is based on energy considerations: the energy release rate G, i.e. the total energy released $\Delta u$ during an interface crack propagation by unit length $\Delta a$ is equal to the work needed to create two new unit crack surfaces. The critical strain energy release rate in Mode II, $G_{IIC}$ (called in the following interfacial fracture toughness, of which the free surface energy is a part) can be derived from experiments, if an accurate description of the stress state, and hence of the energy, is known. In the context of the fragmentation test, this approach has been applied using numerical and analytical methods. In the literature, the prediction of G and $G_{IIC}$ based on a 1-D [1] or a rough 2-D analytical model [2] (with some incorrect assumptions) has been reported for various fibre/matrix systems. Obviously, a high degree of accuracy of either stresses or displacements

predicted by an analytical model is indispensable for an accurate and reliable prediction of G and $G_{IIC}$.

We have previously derived two stress based variational models [3,4], which can predict a rather accurate stress state for two (the fibre and matrix) and three phase system (the fibre, coating and matrix) with a partially debonded (including friction) interface. They have been developed based on the principle of virtual complementary work. Recently, we have also derived an exact expression [5,6] for the energy release rate due to a crack growth. This expression can exactly involve friction work at a rough crack without even using both the displacement and stress distributions at the cracked surfaces as inputs. The sole input for this expression is an accurate stress state or global complementary energy. Using this expression, the two variational models and expression can be readily applied to experimental data, i.e. the fragmentation test data for a highly accurate determination of the interfacial fracture toughness. In this paper, the results of the interfacial fracture toughness for different fibre/matrix systems and a fibre/coating/matrix system with a coating stiffness twice that of the matrix will be presented. Especially it will be shown that the value of the interfacial fracture toughness is strongly influenced by the value of the friction coefficient at the debonded interface, plastic deformation and the accuracy of the models for stress analysis. In addition, some of the fragmentation test results will also be presented.

## CONCEPTS OF FIBRE FRAGMENTATION AND MODEL GEOMETRY

The fragmentation test specimen involves a single fibre embedded into a matrix having a strain to failure at least three times higher than that of the fibre (the left graph of Fig. 1). When the specimen is subject to a monotonically increasing tensile strain, the fibre starts to fracture into fragments within the matrix when the tensile stress (strain) in the fibre is larger than the ultimate strength of the fibre. Then the load is transferred to the broken fibre segments via the shear stress at the interface/interphase. The shear stress transferred in this fashion is equilibrated by a tensile stress in the fibre fragments. This transferred tensile stress, increasing with the increase of the applied strain, when larger than the ultimate strength of the fibre, causes the fibre breaking into smaller segments. Fibre fragmentation continues until the length of the fragment is too short to transfer a load high enough to break the fibre segments. From this moment on, *a saturation level* in the fibre fragment length is reached and the fibre segment will not break any further. The length of the fibre fragment at this threshold is called the critical fibre length, $l_c$. The above process is schematically summarised on the centre and the right graphs of Fig. 1.

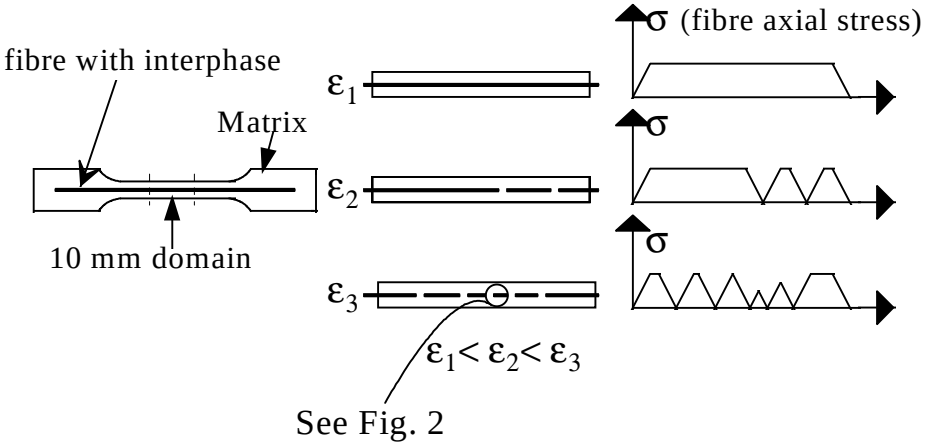


*Fig. 1: The fragmentation test specimen and the development of fragmentation process with the increase of a tensile strain ε along the fibre longitudinal direction*

During the fragmentation process, various kinds of cracks, initiated from the fibre break, can propagate simultaneously with the break of the fibre. These cracks occurs either at the interface or in the matrix. Indeed, depending on the interface and matrix properties, cracks can start off from the fibre/matrix interface for a two phase system or from the fibre/coating or coating/matrix interface for a three phase system, creating a debonding process, or in the matrix in a direction perpendicular to the fibre axis, or at an angle of 45° with respect to the fibre axis. The interface (interphase) debonding is the unique failure phenomenon observed for the two and three phase systems studied in this paper.
During a fragmentation test, the average fragment length and the average debonding ratio at different applied strains are recorded within an observation domain (10mm in this study, see Fig. 1). The debonding ratio is defined as the ratio of the total debonding length to the total fragment length at two adjacent fibre fragments. Both the fragment length and the debonding ratio or length are the input data for the interfacial fracture toughness calculation.

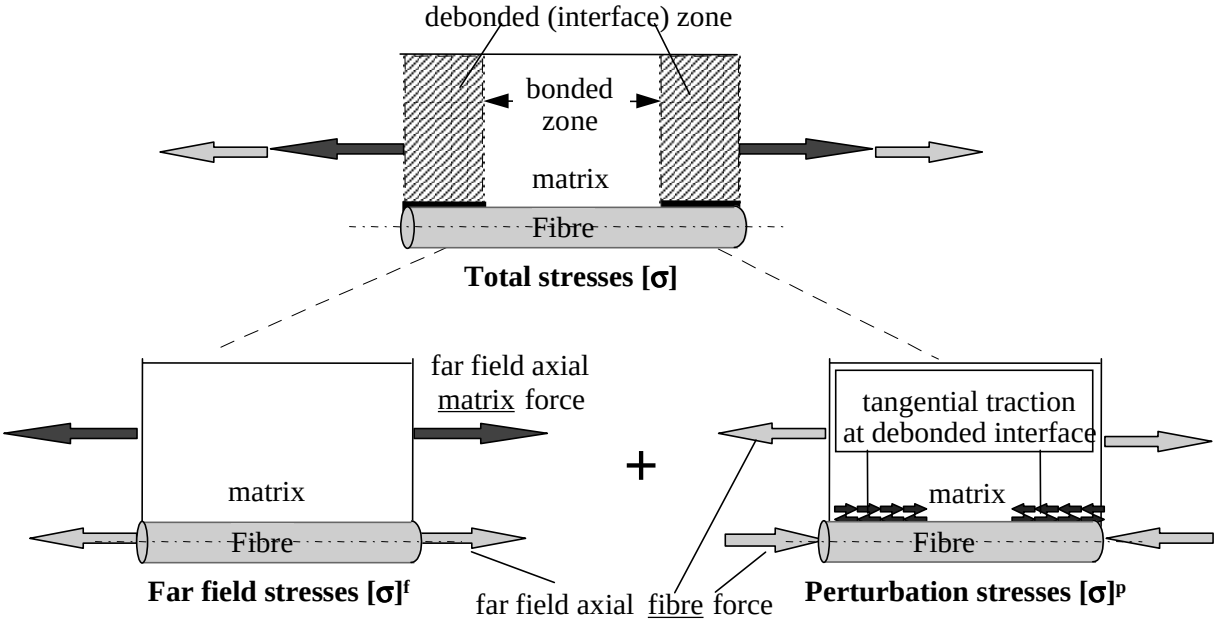


*Fig.2: Model geometry for the stress analysis in a fibre fragment*

The model geometry used for the stress analysis of a fibre fragment is a concentric cylindrical unit (Fig. 2), which is taken from one of the single fibre fragments within the observation domain (10mm in Fig. 1) of a fragmentation test specimen. The fragmentation test samples made in most of the labs have an extremely large ($\rightarrow\infty$) ratio of the matrix radius to the fibre radius.
The general stress expressions everywhere in each phase (cylinder) can be considered as *the superposition* of a far field stress and a perturbation stress (Fig. 2)

$$[\sigma] = [\sigma]^f + [\sigma]^p \tag{1}$$

In Eq. (1), $[\sigma]=(\sigma_{rr}, \sigma_{\theta\theta}, \sigma_{zz}, \tau_{rz})$ is the stress vector in Voigt notation. The stress analysis is axisymmetric. $\sigma_{rr}$, $\sigma_{\theta\theta}$, $\sigma_{zz}$ and $\tau_{rz}$ are the radial, hoop, axial and shear stresses.
By "far field" stresses (indicated by the superscript f in Eq. (1)), we mean *the stress state far away from the fibre crack and debonded interface* in an infinite long fibre.
The "perturbation" stresses (indicated by the superscript p in Eq. (1)), *are local stress variations due to the fibre breaks, the interface debonding or both*.

As shown in Fig. 2, the zero axial force at a fibre break surface can be considered as the superposition of the far field axial force and a negative axial perturbation force (equal to the far field fibre axial force), applied to the intact fibre end face. In the meantime, an equal positive perturbation axial force must be applied to the matrix since the total applied axial load does not change before and after a fibre break. The fibre and matrix surfaces of a debonded interface (with a discontinuous axial displacement) can be considered as a special boundary. The loads on this boundary are a tangential perturbation traction applied to the fibre surface and an equal but opposite traction to the matrix surface.
All the far field stress expressions can be derived, using all interface traction and displacement continuities, from the classical Lamé solution. The far field stresses are exact, i.e. they satisfy both equilibrium and compatibility equations and all the stress and displacement continuities at interfaces. The solution of the perturbation stresses is rather difficult. We have derived two stress based, 2-D variational models [3,4] to predict rather accurate perturbation stresses for two and three phase composites with a partially debonded interface. Using the above-mentioned special boundary condition concept for the debonded interface, the principle of minimum complementary energy can be applied to the whole fragment including the debonded and bonded (interface) zones together so that the strong stress interactions between two zones have been determined rigorously. In this study, both models are used to provide the value of the perturbation complementary or strain energy for calculating the energy release rate using an expression that is presented in the next section.

## THE EXPRESSION OF THE ENERGY RELEASE RATE AND THE CALCULATION FOR THE INTERFACIAL FRACTURE TOUGHNESS

We have recently shown [5,6] that for a n-phase composite subjected to mixed traction-force-displacement boundary conditions and thermal load, the strain energy release rate due to the growth of a friction crack, is the change rate of the total complementary energy , i.e.

$$G = \frac{d}{dA}\left( \sum_{i=1}^{n} \int_{V_i} \frac{1}{2}[\sigma][K][\sigma]dV + \sum_{i=1}^{n} \int_{V_i} [\sigma][\alpha]TdV - \int_{S_D} [P][D]dS \right) \tag{2}$$

where $S_D$ is the part of the boundary surface subjected to prescribed displacements. T is the temperature difference between the room temperature and the stress-free temperature. For the the fragmentation test problem (Fig. 2). it has been further shown [5,6] that the expression of G can be simplified to only the change rate of the perturbation complementary energy $\Gamma^p$

$$G = \frac{d\Gamma^p}{dA} = \frac{d}{dA}\left( \sum_{i=1}^{n} \int_{V_i} \frac{1}{2}[\sigma]^p[K][\sigma]^p dV \right) \tag{3}$$

In Eq. (3), $dA = -4\pi r_1 dl_1$ where $r_1$ is the fibre radius; $l_1$ is the debond length at the half fragment (Fig. 2); $dl_1$ is the debond extension. For the calculation of the interfacial fracture toughness $G_{IIC}$, the input data from the fragmentation test results, as above mentioned, are the average fragment length ($2l$) and the average debonding ratio ($l_1/l$) as a function of the applied strain. For a set of given $l$ and $l_1$ at an applied strain, $d\Gamma^p$ is obtained from the numerical difference of $\Gamma^p$ before and after a very small incremental debond extension $dl_1$, i.e. $d\Gamma^p=\Gamma^p(l, l_1+dl_1)-\Gamma^p(l, l_1)$. In this study, $dl_1$ is set as $0.001r_1$. $G_{IIC}$ at this applied strain can then be calculated from Eq. (3). Using the variational models [3,4] based on the principle of minimum complementary energy, the value of $\Gamma^p$ is the most accurate output.

Thus, a high accurate G (or $G_{IIC}$) can be readily found. Especially, we have shown [5,6] that if the *same tangential traction at the debonded interface* (Fig. 2) is used before and after a very small incremental debond extension $dl_1$, the expression in Eq. (3) can exactly involve friction work caused by the rough debonded surfaces. Since Eq. (3) is the change rate of the global perturbation complementary energy, it appears that G expressed by Eq. (3) is less sensitive to the accuracy of the shear stresses and the axial displacements at the crack surfaces. This feature is very useful, because for most of analytical and FE models, both the displacement and stress distributions at the debonded interface are required as inputs to calculate the friction work but an accurate determination of the stresses and the displacements point by point at a debonded, friction interface is hardly achieved in the zones very close to the fiber crack and the debond tips, even using rigorous 2-D analytical or finite element models.
The detailed calculation procedure for G and $G_{IIC}$ is presented in Refs. [5,6].

## $G_{IIC}$ FOR A COMMERCIALLY TREATED CARBON FIBRE

We now present the results for the interfacial fracture toughness from the test data available in Ref. [7] where the fragmentation test results were summarised as two figures, the average fragment aspect ratio ($l/r_1$) and the average debonding ratio as a function of the applied strain. The fragmentation tests [7] were performed for an intermediate modulus carbon fibre with different surface treatments (SST). The mechanical properties of this carbon fibre and epoxy are provided in Table 1. The curing condition for epoxy is 80°C for 15 hours.

*Table 1: Mechanical properties for 100% SST carbon fibre*

| Property | Carbon fibre | Epoxy matrix |
|---|---|---|
| $E_A$ or $E_m$ (MPa) | 300000 | 3000 |
| $E_T$ (MPa) | 15000 | |
| $G_A$ or $G_m$ | 13700 | 1110 |
| $\nu_A$ or $\nu_m$ | 0.2 | 0.35 |
| $\nu_T$ | 0.35 | |
| $\alpha_A$ or $\alpha_m$ (ppm/°C) | -0.7 | 71.0 |
| $\alpha_T$ (ppm/°C) | 7.0 | |
| diameter (μm) | 5.0 | |
| fibre failure strain | 1.8 % | |
| interface friction coefficient, μ | 0.2-2.0 | |

The notations used in Table 1 for the properties of a transversely isotropic fibre and an isotropic matrix are: $E_A$ and $E_T$ are the axial and transverse modulus of the fibre; $\nu_A$ is the axial and $\upsilon_T$ is the transverse Poisson's ratio of the fibre; $\alpha_A$ and $\alpha_T$ are the axial and transverse thermal expansion coefficients of the fibre; $E_m$ is the modulus, $\nu_m$ is the Poisson's ratio and $\alpha_m$ is the thermal expansion coefficient of the matrix.

As an illustration, we only use from Ref. [7] the data for sample '100% SST' representative of a normal 'strong' interface. Here, we take the data of the debonding ratio and the aspect ratio at three applied strains, 4.2%, 4.4% and 4.6%. We use a little higher strain region, where the dynamic debonding effect (non-stable debonding process) immediately following the fibre break, might be avoided. The friction coefficient μ is unknown and is varied

between 0.2-2.0. The calculated interfacial fracture toughness with different friction coefficients as a function of three applied strain levels are listed in Table 2. The numbers in the brackets of Table 2 are the results predicted by another 2-D model [2] in the literature.
First of all, the fracture toughness is remarkably dependent on the value of the friction coefficient. It is seen from Table 2 that at a certain strain, a higher friction coefficient results in a lower fracture toughness. This tendency is physically reasonable, because a part of the debond driving force (i.e. the total matrix axial force in Fig. 2) has to be consumed to overcome a resistance from the friction tractions (i.e. the tangential perturbation tractions in Fig. 2) at the debonded interface. A higher friction coefficient simply means a higher resistance to be overcome.

*Table 2: Interfacial fracture toughness ($J/m^2$) for sample 100% SST*

| μ | 4.4% | 4.6% | 4.8% |
|---|---|---|---|
| 0.2 | 320 | 352.6 (197.7) | 387 |
| 0.6 | 253.6 | 280.1 (208) | 306.2 |
| 1.0 | 193.5 | 215 (216.2) | 234.4 |
| 2.0 | 74.2 | 86.8 | 95.5 |

Finite element calculations [8,9] in the literature show that for a certain set of applied strain, fragment and debond lengths, the energy release rate G decreases with the increase of μ which confirms our results. However, different FE calculations seem to predict different decrease rates of G with the increase of μ. The FE results by DeBenedetto and Gurvich [8] predict a very slow decrease after $\mu>0.6$ while the FE results by Marotzke [9] predict a decrease rate very similar to that in Table 2. When $\mu<0.6$, the FE results by De Benedetto and Gurvich also agree very well with our analytical results [6]. Much more finite element calculations (with very fine mesh) appear necessary not only for a comparison with the analytical approach but also for judging the accuracy of the FE model itself. Another problem is that the existing FE analyses mainly focused on the calculations of G or $G_{IIC}$ within a rather small range of debond length (typically less than 2xfibre diameter). For both theoretical and practical reasons, FE results for larger debond lengths are also desirable.
The numbers in the brackets of Table 2 show that if a rough 2-D analytical model [2] of fragment stress analysis is used, the tendency might be totally wrong.
Second, the fracture toughness increases slightly (+20%) with the increase of the applied strain. Although the difference between different strains decreases with the increase of the friction coefficient, the general tendency is quite clear, unless one uses a μ much higher than 2.0. According to what has been reported in the literature, μ values above 1.5 seem to be unlikely. Then a problem arises, as from a fracture mechanics analysis, one expects a $G_{IIC}$ nearly independent on the applied strain and crack length. In the present case, this can be explained by the occurrence of plastic deformation. The reason is that after a strain of 4%, substantial plastic deformation occurs in the matrix. As such, a pure $G_{IIC}$ could not be found by the available data. If the friction coefficient is known, the mean value based on the three strains might be used as an approximate estimation, e.g. if $\mu=0.6$, $G_{IIC}$ is about 280 $J/m^2$.

## $G_{IIC}$ FOR AN UNCOATED, UNTREATED CARBON FIBRE AND AN $O_2$-TREATED, PLASMA-COATED CARBON FIBRE

In the framework of a Euram project, a microwave plasma polymerisation process was used to deposit coatings of hexametyldisiloxane (HMDSO). Oxygen was added to alter the composition and morphology of the coating, and hence the mechanical properties (modulus). Coating thicknesses of 0,1 and 0,5 μm were achieved by varying the coating time. Prior to the coating, some of the fibres were plasma-treated under $O_2$-atmosphere (plasma power: 200-600W) because by dynamic observation of the failure (interface debonding) processes during fragmentation tests and by SEM analysis of the transverse sections of test samples, the debonding always occurs at the fibre/coating interface. More details about the process can be found in Ref. [10]. The fibre properties are given in Table 3. The used matrix is the same as that (Table 1) in the previous section. In the following, we present the fragmentation results and calculated $G_{IIC}$ for the samples with two different conditions: (1) the fibres without plasma-treatment and without coating. This type is denoted as pt-/c-; (2) the fibres with plasma-treatment (power: 600W) and with 0.1 μm coating that has a modulus twice that of the matrix. This type is denoted as pt6/c0.1.

*Table 3: Mechanical properties for the carbon fibre and coating*

| Property | Carbon fibre | coating |
|---|---|---|
| $E_A$ or $E_c$(MPa) | 230000 | = 2x$E_m$ |
| $E_T$ (MPa) | 13800 | |
| $G_A$ or $G_c$ (MPa) | 18000 | = 2x$G_m$ |
| $\nu_A$ or $\nu_c$ | 0.2 | = $\nu_m$ |
| $\nu_T$ | 0.37 | |
| $\alpha_A$ or $\alpha_c$ (ppm/°C) | -0.1 | = $\alpha_m$ |
| $\alpha_T$ (ppm/°C) | 10.0 | |
| diameter (μm) | 7 | |
| fibre failure strain | 1.4% | |
| interface friction coefficient, μ | 0.6-1.5 | |
| coating thickness (μm) | 0.1 | |

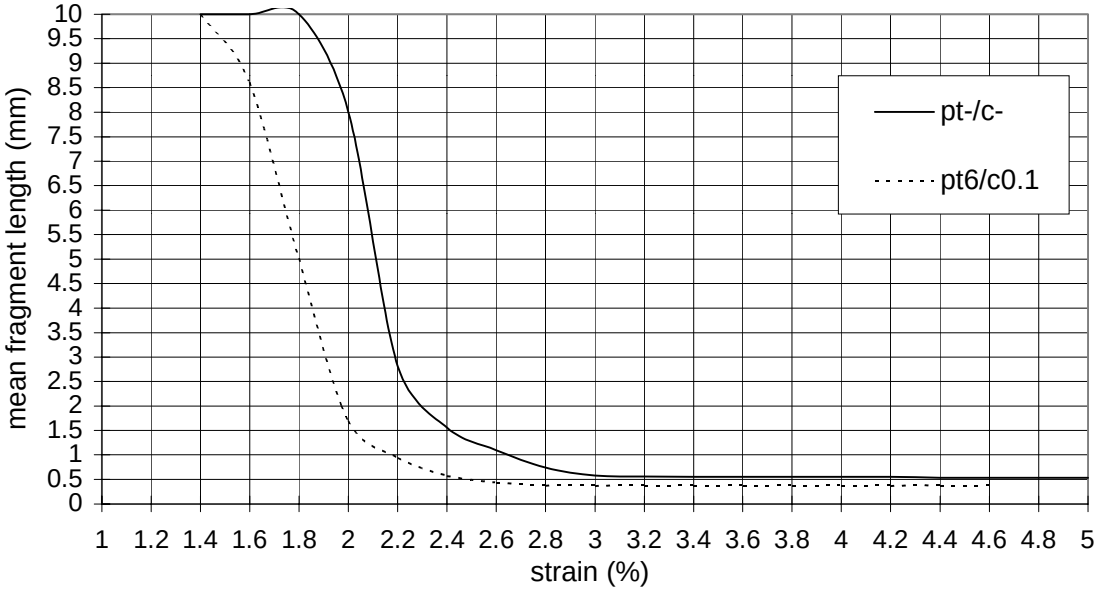


*Fig. 3: Mean profiles of the average fragment length for pt-/c- and pt6/c0.1 samples*

The fragmentation test results were recorded as two types of figures: the average fragment length (Fig. 3) and the average debonding ratio with standard deviation and coefficient of variation (Figs. 4 and 5) as a function of applied strain. In order to exclude the disturbance of plasticity as discussed in the previous section, it appears to be better to use smaller applied strains, despite of the negative influence from the dynamic debonding process. Unfortunately, the big scatter of the test data in Fig. 4 for strains lower than 3.2% prevents such an attempt. The selected applied strains start from 3.2%, after which the data scatter decreases significantly, see the variation of deviation in Fig. 4. This is coincidentally the strain where the fragmentation saturation level is reached. Indeed, it is easier to record an accurate debonding length after the saturation level, because of a smoother debonding growth (without the sudden fibre breaks and consequently dynamic debonding effect). Although the selected applied strains are still high, they are much lower than those in the above case with the same epoxy. Note that while the same epoxy is used, different fibres have been used. Both fibre breaking strain and stiffness for the fibre in Table 3 are lower than those for the fibre in Table 1. Both lower values cause an earlier first fibre break and a lower strain for reaching the saturation level (that a higher fibre stiffness decreases the speed of interface stress transfer has been shown in Ref. [3]). The friction coefficient μ is unknown and is varied between 0.6-1.5, which could be an acceptable range in the literature. The calculated interfacial fracture toughness with different friction coefficients as a function of five applied strain levels are listed in Table 4.

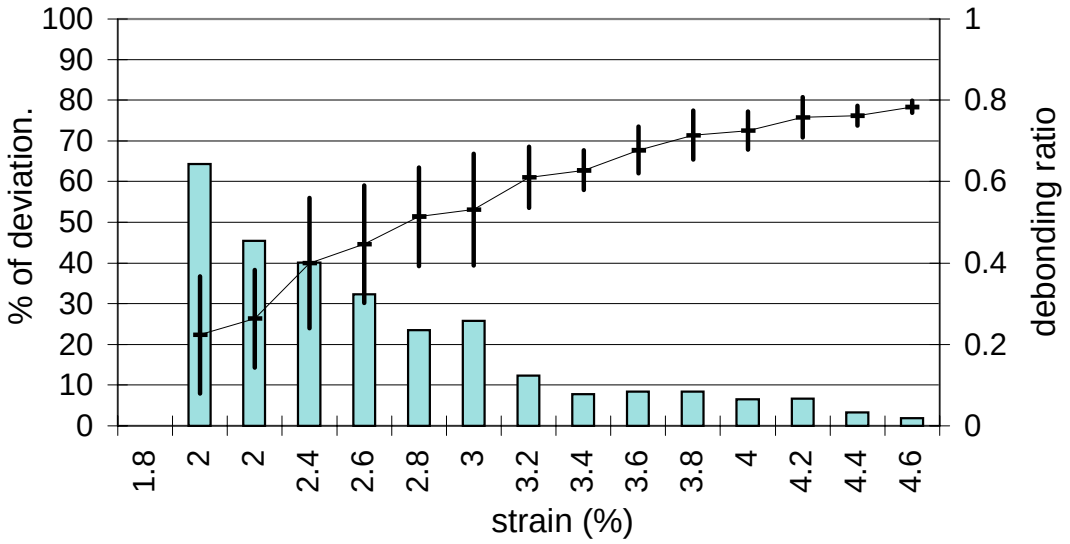


*Fig. 4: Mean profiles of the debonding ratio for samples with condition pt-/c-*

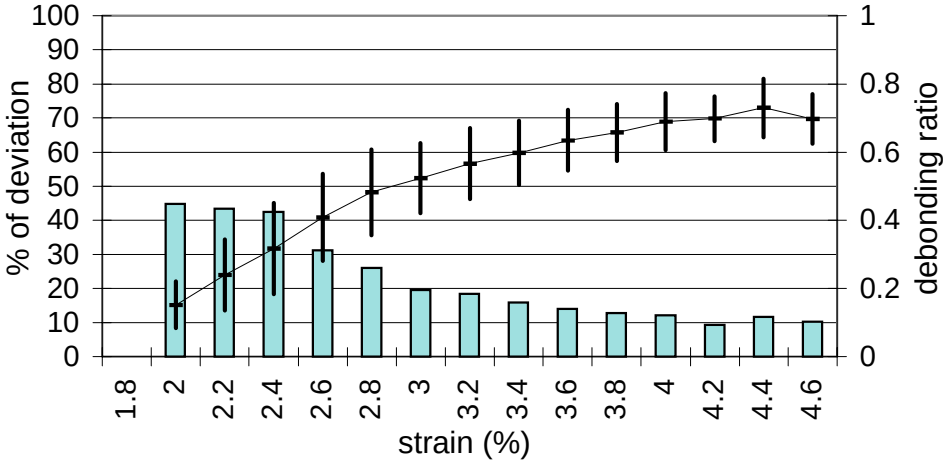


Fig. 5: Mean profiles of the debonding ratio for samples with condition pt6/c0.1

*Table 4: Interfacial fracture toughness ($J/m^2$) for sample pt-/c-*

| μ | 3.2% | 3.4% | 3.6% | 3.8% | 4.2% |
|---|---|---|---|---|---|
| 0.6 | 76.7 | 88 | 95.5 | 101.27 | 118.1 |
| 1.2 | 25.4 | 29.1 | 30.5 | 31.9 | 38.7 |
| 1.5 | 9.6 | 11.75 | 11.9 | 12.1 | 20.0 |

Once again, the fracture toughness is remarkably dependent on the assumed value of the friction coefficient. At a certain strain, a higher friction coefficient causes lower fracture toughness. The fracture toughness increases with the increase of the applied strain but for a μ=1.2 or higher, $G_{IIC}$ can be seen as constant between 3.2% and 3.8%. An absolute constant will rarely be achieved because only few material systems with a crack behave perfectly elastically. A localised plastic deformation always exists around the crack tip, and it usually causes an increased resistance with the crack growth (R-curve effect). The key point here is the value of μ. If it is known, one would be able to estimate the magnitude of the R-curve effect. This also means that it is difficult to conclude that the system has a μ=1.2 only because it gives a nearly constant $G_{IIC}$. We recommend to determine μ independently by other ways such as comparing the interfacial shear stress predicted by the variational models

[3,4] with the experimental Raman spectroscopy results, e.g. Ref. [11]. If one wants to find both $G_{IIC}$ and μ from the fragmentation test, a full simulation of the fragmentation test might be useful. It would also provide more information as different effects such as the position distribution of fibre breaks and dynamic debonding effect at lower, applied strains, are included. The variational models [3,4] with rather accurate stresses can provide a powerful support to such a simulation. Finally it should be noted that for each μ, the $G_{IIC}$ value at an applied strain of 4.2% is much higher than the others. This is due to the predominating plastic deformation which occurs after an applied strain of 4% as discussed above for the results of Table 2.

*Table 5: Interfacial fracture toughness ($J/m^2$) for sample pt6/c0.1*

| μ | 3.2% | 3.4% | 3.6% | 3.8% | 4.2% |
|---|---|---|---|---|---|
| 1.2 | 36.2 | 39.5 | 41.2 | 46.3 | 56.9 |

The exact interfacial fracture toughness for the three phase sample, pt6/c0.1 is more difficult to derive. Besides for the unknown μ, both the thermal expansion coefficient and Poisson's ratio of the coating are also not yet available. Hence only the results based on a μ=1.2 is provided in Table 5 for a relative comparison with the two-phase sample results in Table 4. Both the thermal expansion coefficient and Poisson's ratio for the matrix are assumed also for the coating (Table 3).
The same tendency as the corresponding values in Table 4 is seen but the values in Table 5 are higher. This at least means that the HMDSO plasma coating/fibre interface has a relatively higher fracture toughness than the untreated fibre/matrix interface, *after a strong $O_2$ pretreatment*.

## CONCLUSION

An expression [5,6] suited for a more accurate calculation of the energy release rate from a stress based model is presented. This expression, associated with the two partially debonded-interface models [3,4], yields a rather reliable prediction for the strain energy release rate due to the growth of an interface crack in a 2- or 3-phase composite under thermoelastic loading. In particular, this expression takes the frictional work at the debonded interface into account. The interfacial fracture toughness $G_{IIC}$ is strongly dependent on the value of the friction coefficient at the debonded interface. Thus, it is proposed to have other independent ways to derive the friction coefficient. Otherwise, a complete test simulation might be required. The stress analysis model used for providing the value of strain or complementary energy is also critical for the accuracy of $G_{IIC}$. In addition, the plastic deformation plays a marked role in the high strain region.

## REFERENCES


1. Liu, H. Y., Mai, Y. W., Zhou, L. M. and Ye, L., "Simulation of the fibre fragmentation process by a fracture mechanics analysis", *Composites Science and Technology*, Vol.52, 1994, pp. 253-260.
2. Copponnex, T. J., "Analysis and evaluation of the single-fibre fragmentation test", *Composites Science and Technology*, Vol.56, 1996, pp. 893-909.
3. Wu, W., Verpoest, I. and Varna, J., "A novel axisymmetric variational analysis of the stress transfer into fibre through a partially debonded interface", *Composites Science and Technology*, Vol.58, 1998, pp. 1863-1877.
4. Wu, W., Jacobs, E., Verpoest, I. and Varna, J., "Variational approach to the stress transfer problem through partially debonded interfaces in a three phase composite", *Composites Science and Technology*, Vol.59, 1999, pp. 519-535.
5. Wu, W., "Stress transfer through the fibre-matrix interphase in axially loaded composites", Ph.D dissertation, K.U.Leuven, Leuven, Belgium, March, 1999.
6. Wu, W., Verpoest, I. and Varna, J., "Prediction of energy release rate due to the growth of an interface crack by variational analysis", submitted to *Composites Science and Technology*, January, 1999.
7. Lacroix, th., Keunings, R., Desaeger, M. and Verpoest, I., "A new data reduction scheme for the fragmentation testing of polymer composites", *Journal of Materials Science*, Vol.30, 1995, pp. 683-692.
8. DeBenedetto, A. T. and Gurvich, M. R., "Effect of friction between fiber and matrix on the fracture toughness of the composite interface", *Journal of Materials Science*, Vol.33, 1998, pp. 4239-4248.
9. Marotzke, C., "Analysis of singularities and interfacial crack propagation in micromechanical tests", *Proceeding of the first international conference on damage and failure of interface (DFI-1)*, Vienna, Austria, September 22-24, 1997, Damage and Failure of Interfaces, Rossmanith, H. P., Ed., pp. 365-372.
10. Kettle, A. P., Jones F. R., Alexander, M. R. (U.K), Stollenwerk M. (Germany), Wu, W., Jacobs, E. and Verpoest, I. (Belgium), "Experimental evaluation of interphase region for carbon fibre composite with plasma polymerised coating", *Composites Part A*, Vol.29A, 1998, pp. 241-250.
11. Melanitis, N., Galiotis C., Tetlow, P. L. and Davies, C. K. L., "Monitoring the micromechanics of reinforcement in carbon fibre/epoxy resin systems", *Journal of Materials Science*, Vol.28, 1993, pp. 1648-1654.